NONLINEAR SOIL-STRUCTURE INTERACTION ANALYSIS WITH SUBSTRUCTURING METHOD

Behtash JAVIDSHARIFI
Construction Superintendent, Fars Regional Electricity Company, Shiraz, Iran
b.javidsharifi@sutech.ac.ir

Hossein RAHNEMA
Assistant Professor, Shiraz University of Technology, Shiraz, Iran
rahnema@sutech.ac.ir

Sassan MOHASSEB
Professor, Tehran University, Tehran, Iran
smteam@gmx.ch

Keywords: Soil-Structure Interaction, Substructuring, Nonlinearity, Constitutive Model, Structural Responses

ABSTRACT

Soil-structure interaction (SSI) has been inspected through various methods so far. One simple and effective way of formulating the problem is using substructures, yet the superposition done in this approach yields to linear assumption of the interactional responses, while it is contrary to the reality. To reach more practical responses, manipulations can be done to the substructuring method to generalize the results to the nonlinear case, which leads to more realistic results based on which more exact engineering judgements can be performed. Instead of assuming the foundation-underlying soil to react like linearly-behaving springs, Terzaghi's ultimate bearing capacity concept through the UCD model is supposed adjoining this substructure. The springs replacing the soil will react linearly only to a level of incoming loads, and will enter their nonlinear phase after a threshold. The structure is supposed to be a reinforced concrete frame placed upon shallow footings. The input motion is the seismic load derived from the Loma Prieta earthquake (1989). Properties corresponding to different densities of sand, namely loose (15% < Dr < 35%), medium dense (65% < Dr < 85%) and dense (Dr > 35%) are examined. Modelling is done using the OpenSees software with programming in the Active Tcl environment. Maximum displacements of the structure and base reactions considering nonlinear seismic SSI are recorded and compared with a study previously done in Turkey using Plaxis. Average displacements of stories for all densities of sand are less for the UDC model compared to those from the Mohr-Coulomb. Denser sand results in base shears slightly bigger than those of sands with other density states.

INTRODUCTION

For more than a century researchers have been aware of the impact of the underlying soil on structural responses. The studies began primarily with inspecting static effects and settlements of the structure along with stress distribution caused by the superstructure loads through the soil. It was soon discovered that it is especially during dynamic loadings that the underlying soil shows itself off and can be entangling to engineers. To inspect the effects of the soil, one common approach is to model the soil with springs and dashpots under the structure, which is called *substructuring* method. The substructures are modelled as a series of springs and dashpots in parallel and serial and their locations are chosen to fit the system characteristics best. Soil-structure interaction through substructures in time and frequency domains is described in full details by Wolf (1965, 1988). Figure 1 depicts a simple model taking up this approach.

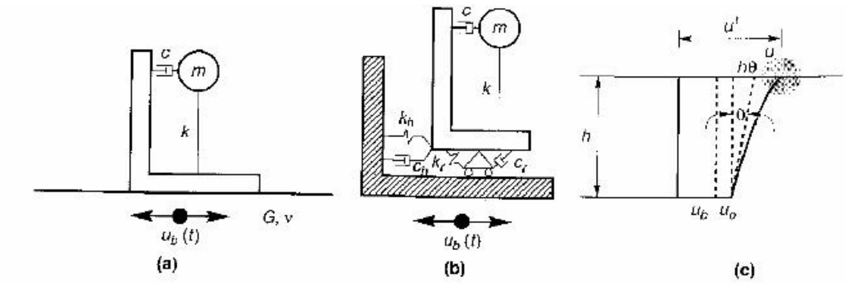

Figure 1. Substructuring method of SSI analysis (after Wolf, 1985)

The total displacement then would be calculated as in Eq. (1):

$$u^t = u_b + u_o + h\theta + u \tag{1}$$

where *u*'s can be observed on Figure 1. Since superposition is performed in this approach, no nonlinearity is assumed in the solution. To overcome this shortcoming, the behaviour of the soil-replacing springs may be addressed which is shown schematically in Figure 2.

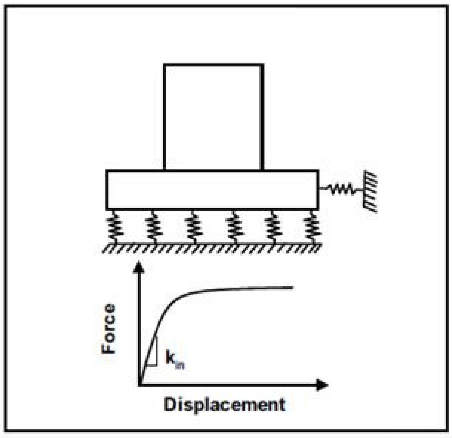

Figure 2. Substructuring method of SSI analysis with nonlinearly behaving springs
(after Raychowdhury and Hutchimson, 2008)

In order to account for the softening of the soil in high strains which cause the nonlinearity, the UCD[1] soil model is implemented. To use this model in the present solution scheme, conventional fundamentals of shallow foundations bearing capacity have been used as in Eq. (2) (Terzaghi, 1943):

$$q_{ult} = cN_cF_{cs}F_{cd}F_{ci} + \gamma D_f N_q F_{qs}F_{qd}F_{qi} + 0.5\gamma B N_\gamma F_{\gamma s}F_{\gamma d}F_{\gamma i} \tag{2}$$

where q_{ult} is the ultimate bearing capacity for unit area of the footing; *c* is the cohesion of the underlying soil of the foundation in case cohesive; *B* dimension of the foundation and N_c, N_q and N_r are bearing capacity factors. F_{cs}, F_{cd} and F_{ci} are supposed shape, F_{qs}, F_{qd} and F_{qi} depth and F_{rs}, F_{rd} and F_{ri}, inclination factors in each section of the equation. The lateral bearing capacity is calculated as the total resisting force on the embedded side of the footing, as in Eq. (3):

$$p_{ult} = 0.5 ¥ K_p D_f^2 \tag{3}$$

1- University of California Davis

in which p_{ult} is the soil passive pressure in unit area and K_p is the passive lateral pressure coefficient based on Coulomb (1776). The structure is then supposed to be placed on such springs through its footings as illustrated in Figure 3.

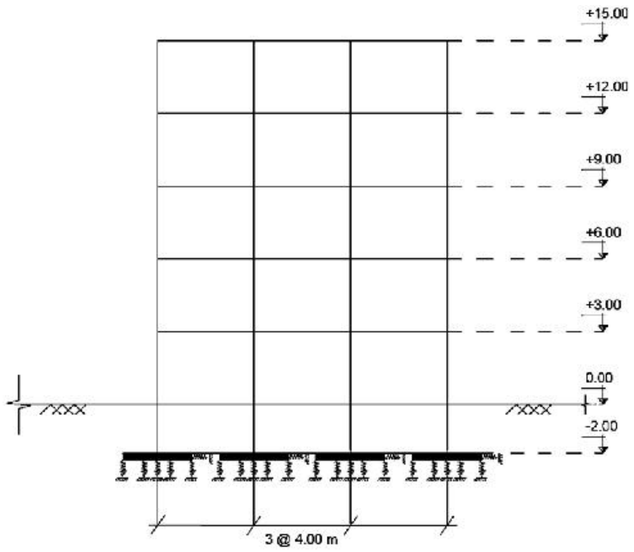

Figure 3. Structure placed on soil-replacing springs

Since nonlinear responses of the whole system are to be recorded, the potential needs to be provided for all elements and materials of the media, including frame elements. The superstructure is supposed to be a reinforced concrete frame which has been provided with such capability. Fig. 4 depicts the cross section of all beam and column elements so as to provide the stiffness and cross section area of the elements in Çelebi et al. (2012).

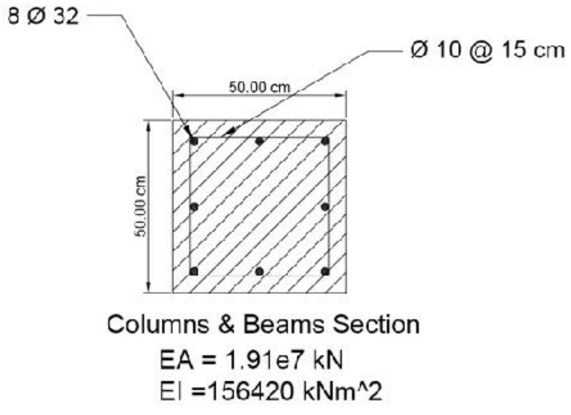

Figure 4. Beam and column elements cross section

Mechanical properties of structural materials are presented in Tables 1 and 2.

Table 1. Mechanical properties of concrete for non-linear structural behaviour

Mechanical Properties	Characteristic Strength (kPa)	Strain in Maximum Strength	Crushing Strength (kPa)	Strain before Crushing	Tension Strength (kPa)
Core Concrete	24×10^3	0.0024	5.6×10^3	0.015	0
Cover Concrete	21×10^3	0.002	5×10^3	0.005	0

Table 2. Mechanical properties of steel for non-linear structural behaviour

Mechanical Properties	Yield Stress (kPa)	Initial Modulus of Elasticity (kPa)	Strain Hardening Ratio
Reinforcing Steel	420×10^3	2×10^8	0.01

The geometry of the RC frame, as was schematically illustrated in Figure 3, is presented in Table 3.

Table 5. Geometric properties of the RC frame

Number of Stories	Typical Story Height (m)	Basement Story Height (m)	Number of Intervals	Length of Intervals (m)	Foundation Rigidity Measure	Load per Unit Length of Beam Elements (kNm^{-1})
6	3	2	3	4	Rigid	50

Soil properties, based on which underlying springs are derived are shown in Table 6.

Table 6. Values of sand mechanical properties in different density states

	Loose Sand (D_r = 15%-35%)	Medium-dense Sand (D_r = 65%-85%)	Dense Sand (D_r = 85%-100%)
Density (ton/m^3)	1.7	2.0	2.1
Reference shear modulus at $p_r' = 80$ (kPa)	5.5×10^4	1.0×10^5	1.3×10^5
Reference bulk modulus at $p_r' = 80$ (kPa)	1.5×10^5	3.0×10^5	3.9×10^5
Friction angle (degrees)	29	37	40
Peak shear strain at $p_r' = 80$ (kPa)	0.1	0.1	0.1
Reference pressure (p_r')	80	80	80
Pressure dependence coefficient	0.5	0.5	0.5
Phase transformation angle (degrees)	29	27	27
Porosity (e)	0.85	0.55	0.45

Loma-Prieta earthquake (1989) record has been chosen as having suitable characteristics of general earthquake records to perform time-history analyses. Horizontal and vertical motions of this earthquake record are depicted in Figures 4 and 5.

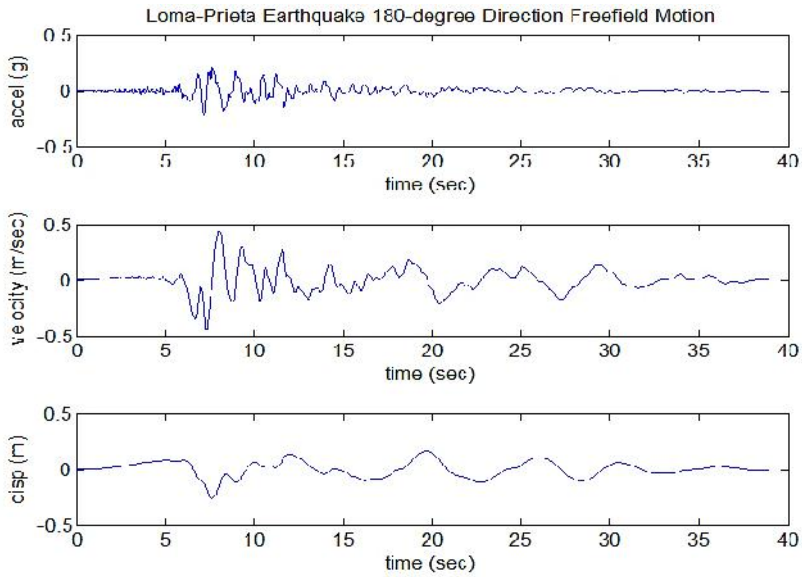

Figure 4. Acceleration, velocity and displacement time histories of free-field NS component of Loma Prieta recorded during the 1989 earthquake, scaled to g

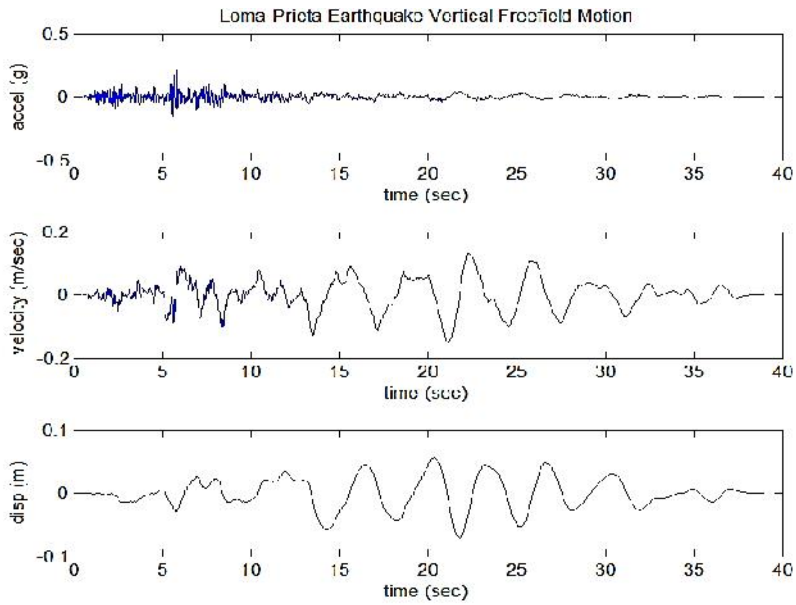

Figure 5. Acceleration, velocity and displacement time histories of free-field vertical component of Loma Prieta recorded during the 1989 earthquake, scaled to g

After the structure was modelled and placed on the nonlinear springs, the earthquake motion was exerted to the base level of the structure, which was 2 meters below the ground surface. Peak displacements of the stories were recorded and plotted as can be seen in Figure 6. It should be noted that the force-depending stiffness of the imaginary springs is calculated based on the density of the underlying soil, meaning that analyses are done for different density states resulting in different springs each time.

Amongst the above-drawn curves, the ones representing responses of linear structure on elastic base, linear structure on non-linear foundation and non-linear structure on non-linear foundation are most informative. It can be inferred from these curves that for the linear elastic frame, which is mostly the case subject to medium intensity earthquakes when designing of commonplace structures has been performed based on current codes, on a non-linear inelastic foundation which accounts for the highly probable non-linearity of soils, structural response amplitudes may vary between those of totally elastic and totally inelastic systems. Compared to the linear fixed-base structure, on the other hand, a shift of about 2 centimeters is observed for all stories other than the basemat which seems to tend to remain constant in the height of the structure. On the basis of this comparison, the non-linear fixed-base frame, which does not seem to be logical though a common assumption, underestimates responses for heights less than 4 meters while shows overestimation for heights more than this. It should not be neglected that although the green curve is like an average-push of the five different possible structural responses, conservatively the closest curve to reality is that of the totally non-linear system and hence all other simulations more or less yield underestimation when compared to this curve.

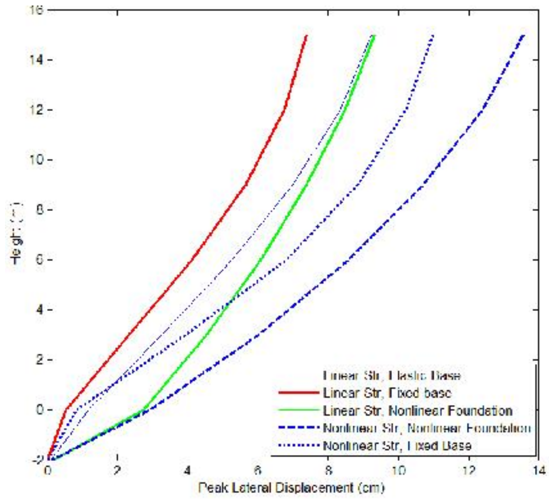

Figure 6. Frame displacement amplitudes when loose sand exists under the foundation

Medium-dense sand properties were also examined once and responses are illustrated in Figure 7.

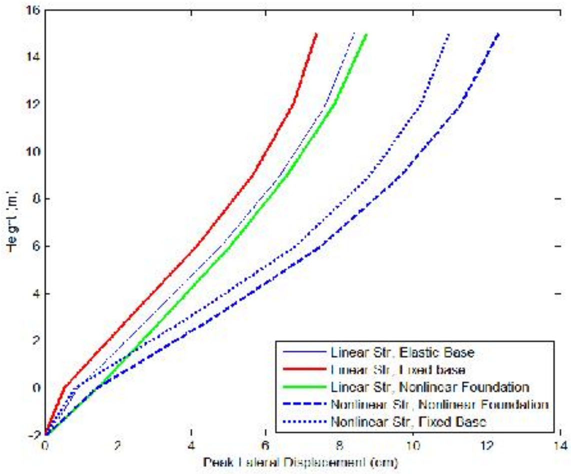

Figure 7. Frame displacement amplitudes when medium-dense sand exists under the foundation

Apparently, as the height increases, not only displacements get larger but also the gap between amplitudes of linear frames and non-linear ones grows bigger and for the totally non-linear systems gets more critical. Figure 19 represents the same issue for the case of dense sand. It is observed that the denser the soil, the less SSI perceived, and SSI is least comprehensible for the densest state of sand existing under and around the basemat.

It is worthwhile mentioning that although the difference of response amplitudes for the linear fixed-base system and the totally non-linear one is something between 4 to 8 centimeters in the top story of the frame for all sand densities and compaction states, this amount may be controlling as it may govern the target displacement of the structure when performance-based design of the building is of interest.

For the case of dense sand, peak structural responses are presented in Figure 8.

For the sake of comparison, resulting structural displacements for the frame placed on medium and stiff clays are presented in Figures 9 and 10.

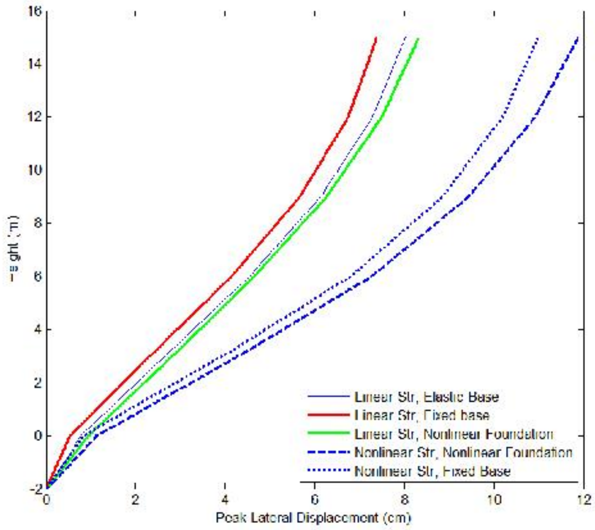

Figure 8. Frame's displacement amplitudes in its height for dense UCD sand under the foundation

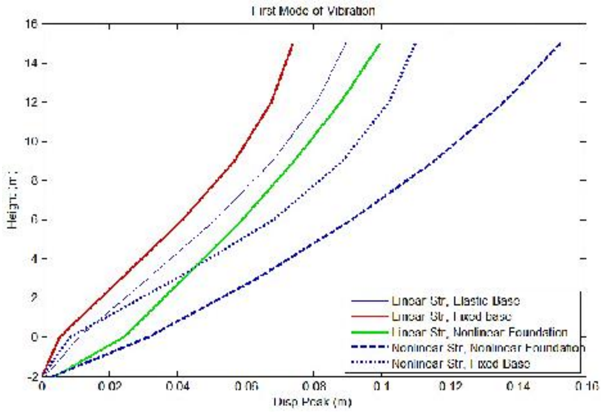

Figure 9. Frame's displacement amplitudes in its height for medium UCD clay under the foundation

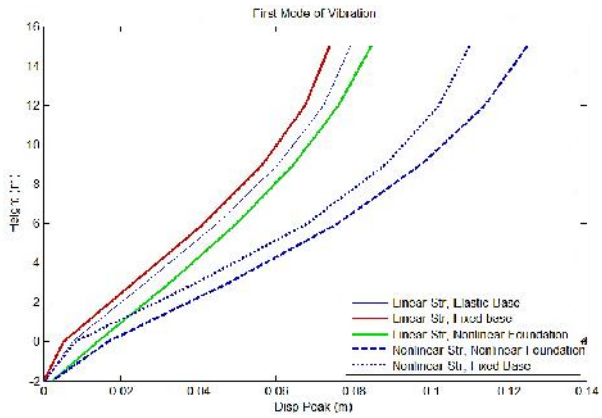

Figure 9. Frame's displacement amplitudes in its height for stiff UCD clay under the foundation

CONCLUSIONS

A reinforced concrete frame was modelled on potentially elastoplastic sandy soil. The constitutive model UCD was inserted for modelling the behaviour of the soil, for the purpose of non-linear sub-structuring. Firstly, it is obvious that the linear substructuring method has got no more reason to be performed since more exact solutions which are quite easy at the same time exist. A small manipulation in the behavior of the springs yields responses much closer to reality. Results of the nonlinear cases seemingly depend on the density of the soil which is accounted for by the mechanical properties of the substituting springs, which in turn depend on the density of the soil they are replacing. As the soil gets denser displacements get closer to those of the elastic base case. Maximum displacements of the structure on elastoplastic soil are shown in Table 7 for the sake of comparison.

Table 7. Maximum displacements of the structure on elastoplastic soil with different constitutive models (m)

Height (m)	Mohr-Coulomb, low compaction	Mohr-Coulomb, medium compaction	Mohr-Coulomb, high compaction	UCD, low compaction	UCD, medium compaction	UCD, high compaction
-2	-	-	-	0	0	0
0	0	0	0	0.025	0.015	0.013
3	0.082	0.038	0.028	0.057	0.052	0.028
6	0.168	0.077	0.067	0.104	0.075	0.071
9	0.240	0.115	0.105	0.122	0.099	0.088
12	0.292	0.148	0.136	0.139	0.121	0.108
15	0.325	0.168	0.156	0.149	0.134	0.118

The importance of the nonlinearization of the structure base lies in the changes of probable destruction patterns which results from different relative displacements of the structure stories. This issue is inspected and represented in a parallel work.

ACKNOWLEDEMENTS

The authors wish to thank Dr. A. H. Baghlani's invaluable guidelines for time domain analyses. This study was carried out under the support of Shiraz University of Technology for the proceedings of the 7th International Conference on Seismology & Earthquake Engineering. Reviewers are to be thanked gratefully for their insight into the matter and their kind remarks.

REFERENCES

Çelebi E, Göktepe F and Karahan N (2012) Non-linear finite element analysis for prediction of seismic response of buildings considering soil-structure interaction. Natural Hazards & Earth System Sciences, 12(11)

Clough RW and Penzien J (1993) Dynamics of Structures, 2nd Ed., McGraw-Hill Book Company, New York

Handin J (1969) On the Coulomb-Mohr failure criterion. Journal of Geophysical Research, 74(22): 5343-5348

Raychowdhury P (2008) Nonlinear winkler-based shallow foundation model for performance assessment of seismically loaded structures, ProQuest

Terzaghi K (1943) Theoretical soil mechanics

Wolf JP (1985) Dynamic soil-structure interaction, Prentice Hall Int